THE JOURNAL OF BIOLOGICAL CHEMISTRY VOL. 284, NO. 23, pp. 15541–15548, June 5, 2009

Signaling Processes for Initiating Smooth Muscle Contraction upon Neural Stimulation*

Received for publication, February 6, 2009, and in revised form, March 30, 2009 Published, JBC Papers in Press, April 6, 2009, DOI 10.1074/jbc.M900888200

Hai-Lei Ding, Jeffrey W. Ryder[1], James T. Stull, and Kristine E. Kamm[2]

From the Department of Physiology, University of Texas Southwestern Medical Center, Dallas, Texas 75390

Relationships among biochemical signaling processes involved in Ca^{2+}/calmodulin (CaM)-dependent phosphorylation of smooth muscle myosin regulatory light chain (RLC) by myosin light chain kinase (MLCK) were determined. A genetically-encoded biosensor MLCK for measuring Ca^{2+}-dependent CaM binding and activation was expressed in smooth muscles of transgenic mice. We performed real-time evaluations of the relationships among $[Ca^{2+}]_i$, MLCK activation, and contraction in urinary bladder smooth muscle strips neurally stimulated for 3 s. Latencies for the onset of $[Ca^{2+}]_i$ and kinase activation were 55 ± 8 and 65 ± 6 ms, respectively. Both increased with RLC phosphorylation at 100 ms, whereas force latency was 109 ± 3 ms. $[Ca^{2+}]_i$, kinase activation, and RLC phosphorylation responses were maximal by 1.2 s, whereas force increased more slowly to a maximal value at 3 s. A delayed temporal response between RLC phosphorylation and force is probably due to mechanical effects associated with elastic elements in the tissue. MLCK activation partially declined at 3 s of stimulation with no change in $[Ca^{2+}]_i$ and also declined more rapidly than $[Ca^{2+}]_i$ during relaxation. The apparent desensitization of MLCK to Ca^{2+} activation appears to be due to phosphorylation in its calmodulin binding segment. Phosphorylation of two myosin light chain phosphatase regulatory proteins (MYPT1 and CPI-17) or a protein implicated in strengthening membrane adhesion complexes for force transmission (paxillin) did not change during force development. Thus, neural stimulation leads to rapid increases in $[Ca^{2+}]_i$, MLCK activation, and RLC phosphorylation in phasic smooth muscle, showing a tightly coupled Ca^{2+} signaling complex as an elementary mechanism initiating contraction.

Increases in $[Ca^{2+}]_i$[3] in smooth muscle cells lead to Ca^{2+}/CaM-dependent MLCK activation and RLC phosphorylation. Phosphorylation of RLC increases actin-activated myosin MgATPase activity leading to myosin cross-bridge cycling with force development (1–3).

The activation of smooth muscle contraction may be affected by multiple cellular processes. Previous investigations show that free Ca^{2+}/CaM is limiting for kinase activation despite the abundance of total CaM (4–6). The extent of RLC phosphorylation is balanced by the actions of MLCK and myosin light chain phosphatase, which is composed of three distinct protein subunits (7). The myosin phosphatase targeting subunit, MYPT1, in smooth muscle binds to myosin filaments, thus targeting the 37-kDa catalytic subunit (type 1 serine/threonine phosphatase, PP1c) to phosphorylated RLC. RLC phosphorylation and muscle force may be regulated by additional signaling pathways involving phosphorylation of RLC by Ca^{2+}-independent kinase(s) and inhibition of myosin light chain phosphatase, processes that increase the contraction response at fixed $[Ca^{2+}]_i$ (Ca^{2+}-sensitization) (8–14). Many studies indicate that agonist-mediated Ca^{2+}-sensitization most often reflects decreased myosin light chain phosphatase activity involving two major pathways including MYPT1 phosphorylation by a Rho kinase pathway and phosphorylation of CPI-17 by PKC (8, 14–16). Additionally, phosphorylation of MLCK in its calmodulin-binding sequence by a Ca^{2+}/calmodulin-dependent kinase pathway has been implicated in Ca^{2+} desensitization of RLC phosphorylation (17–19). How these signaling pathways intersect the responses of the primary Ca^{2+}/CaM pathway during physiological neural stimulation is not known.

There is also evidence that smooth muscle contraction requires the polymerization of submembranous cytoskeletal actin filaments to strengthen membrane adhesion complexes involved in transmitting force between actin-myosin filaments and external force-transmitting structures (20–23). In tracheal smooth muscle, paxillin at membrane adhesions undergoes tyrosine phosphorylation in response to contractile stimulation by an agonist, and this phosphorylation increases concurrently with force development in response to agonist. Expression of nonphosphorylatable paxillin mutants in tracheal muscle suppresses acetylcholine-induced tyrosine phosphorylation of paxillin, tension development, and actin polymerization without affecting RLC phosphorylation (24, 25). Thus, paxillin phosphorylation may play an important role in tension development in smooth muscle independently of RLC phosphorylation and cross-bridge cycling.

Specific models relating signaling mechanisms in the smooth muscle cell to contraction dynamics are limited when cells in tissues are stimulated slowly and asynchronously by agonist diffusing into the preparation. Field stimulation leading to the rapid release of neurotransmitters from nerves embedded in the tissue avoids these problems associated with agonist diffusion (26, 27). In urinary bladder smooth muscle, phasic contrac-

* This work was supported, in whole or in part, by National Institutes of Health Grant HL26043. This work was also supported by the Moss Heart Fund and the Fouad A. and Val Imm Bashour Distinguished Chair in Physiology (to J. T. S.).

[1] Current address: Universities Space Research Association, NASA Johnson Space Center, 2101 NASA Parkway, Mail Code SK3, Houston, TX 77058.

[2] To whom correspondence should be addressed. Tel.: 214-645-6036; Fax: 214-645-6049; E-mail: kristine.kamm@utsouthwestern.edu.

[3] The abbreviations used are: $[Ca^{2+}]_i$, intracellular Ca^{2+}; CaM, calmodulin; MLCK, smooth muscle myosin light chain kinase; RLC, myosin regulatory light chain; FRET, fluorescence resonance energy transfer; MYPT1, myosin phosphatase targeting subunit-1; PKC, protein kinase C; CPI-17, PKC-potentiated phosphatase inhibitor.

tions are brought about by the parasympathetic nervous system. Upon activation, parasympathetic nerve varicosities release the two neurotransmitters, acetylcholine and ATP, that bind to muscarinic and purinergic receptors, respectively. They cause smooth muscle contraction by inducing Ca^{2+} transients as elementary signals in the process of nerve-smooth muscle communication (28–30). We recently reported the development of a genetically encoded, CaM-sensor for activation of MLCK. The CaM-sensor MLCK contains short smooth muscle MLCK fused to two fluorophores, enhanced cyan fluorescent protein and enhanced yellow fluorescent protein, linked by the MLCK calmodulin binding sequence (6, 14, 31). Upon dimerization, there is significant FRET from the donor enhanced cyan fluorescent protein to the acceptor enhanced yellow fluorescent protein. Ca^{2+}/CaM binding dissociates the dimer resulting in a decrease in FRET intensity coincident with activation of kinase activity (31). Thus, CaM-sensor MLCK is capable of directly monitoring Ca^{2+}/CaM binding and activation of the kinase in smooth muscle tissues where it is expressed specifically in smooth muscle cells of transgenic mice. We therefore combined neural stimulation with real-time measurements of $[Ca^{2+}]_i$, MLCK activation, and force development in smooth muscle tissue from these mice. Additionally, RLC phosphorylation was measured precisely at specific times following neural stimulation in tissues frozen by a rapid-release electronic freezing device (26, 27). Results from these studies reveal that physiological stimulation of smooth muscle cells by neurotransmitter release leads to rapid increases in $[Ca^{2+}]_i$, MLCK activation, and RLC phosphorylation at similar rates without the apparent activities of Ca^{2+}-independent kinases, inhibition of myosin light chain phosphatase, or paxillin phosphorylation. Thus, the elemental processes for phasic smooth muscle contraction are represented by this tightly coupled Ca^{2+} signaling complex.

EXPERIMENTAL PROCEDURES

Preparation of Urinary Bladder Smooth Muscle Strips from Mice—Transgenic mice with CaM-sensor MLCK expression specifically in smooth muscle tissues were bred and screened as previously described (6). Expressed amounts of the MLCK CaM-sensor were less than 30% of the content of endogenous kinase and stresses generated by bladder strips from wild-type and transgenic animals were comparable (6). Transgenic animals showed no obvious phenotypic differences from wild-type mice. All animal protocols were approved by the University of Texas Southwestern Medical Center IACUC.

Mouse bladder tissues were obtained from 8–12-week-old transgenic mice expressing CaM-sensor MLCK or age-matched wild-type mice. Briefly, the urinary bladder was removed, opened, and urothelium removed by blunt dissection. The smooth muscle layer was dissected into longitudinal strips ($0.5 \times 0.5 \times 8.0$ mm) that were mounted on a fluorescence myograph (Scientific Instruments, Heidelberg, Germany) or an isometric force apparatus. Strips were equilibrated and stretched 1.2 times slack length. All protocols were performed in physiological salt solution (in mM: 118.5 NaCl, 4.75 KCl, 1.2 $MgSO_4$, 1.2 KH_2PO_4, 24.9 $NaHCO_3$, 1.6 $CaCl_2$, 10.0 D-glucose, pre-gassed with 95% O_2, 5% CO_2 at 35 °C).

Simultaneous Measurement of Contraction and CaM-Sensor MLCK FRET Ratio or $[Ca^{2+}]_i$—Simultaneous measurements of force and FRET ratio or $[Ca^{2+}]_i$ were made as previously described (6). Because of the potential for CaM-sensor fluorescence to interfere with the fluorescence of Indo-1 in muscle strips and the potential for overexpressed green fluorescent protein containing proteins to interfere with muscle contraction by interacting with myosin (32), we determined that there was no difference in the latency of force development between wild-type and CaM-sensor transgenic mice (data not shown). These data are consistent with previous analyses on force development with the agonist carbachol and KCl (6). FRET ratio, $[Ca^{2+}]_i$, and force measurements were recorded on a Powerlab 8/SP data acquisition unit (AD Instruments, Colorado Springs, CO). For FRET measurements, the muscle strips were illuminated with an excitation wavelength of 430 nm, and emission light was detected by two photomultipliers using 480- and 525-nm filters. The extent of MLCK activation was determined from the 480/525-nm emission ratio (FRET ratio) for strips electrically stimulated with conditions (50 Hz, 20 V, 0.5-ms duration) that induce maximal muscle contraction. Strips were stimulated at 5-min intervals for up to 20 times to collect data for signal averaging.

Global intracellular calcium concentrations were measured by the Indo-1 fluorescence ratio in wild-type bladder strips as described previously (6). Bladder smooth muscle strips were incubated in the dark with physiological salt solution containing 10 μM Indo-1 AM, 0.01% pluronic F-127, and 0.02% cremophor for 4 h at room temperature. After incubation, tissues were mounted in the fluorescence myograph and washed with fresh physiological salt solution for 30 min at 35 °C. Strips were illuminated at 365 nm and emission intensities were measured at 405 and 485 nm to obtain an emission ratio of 405 to 485 nm. Strips were stimulated as for FRET measurements.

Fluorescence ratio data were analyzed over the course of a contraction-relaxation cycle with 50 Hz stimulation for 3 s followed by 12 s relaxation (Fig. 1). To improve signal-to-noise and retain temporal resolution, unfiltered signals were averaged (8–20 contractions from a single strip) after alignment to the initial stimulus pulse using a signal-averaging program written for Matlab. Latency for an increase in the fluorescence ratio was estimated as the time after stimulus initiation at which the signal no longer oscillated below the mean of the average resting value.

Preparation of Electrically Stimulated Bladder Smooth Muscle Strips for Biochemical Measurements—Strips of bladder smooth muscle were dissected and mounted by silk thread to Grass FT03 force transducers for measurement of isometric force. Fine silver wire attached directly to the ends of the tissue allowed continuous field stimulation of the preparation between the time the organ bath was lowered and the tissue was frozen. After mounting, strips were equilibrated, stretched to optimal length, and pre-contracted with 65 mM KCl. Strips remained quiescent for at least 30 min and were frozen immediately following 0, 100, 250, 1200, or 3000 ms of 50 Hz electric field stimulation. Force development was recorded on a Powerlab 8/SP data acquisition unit (AD Instruments, Colorado Springs, CO). Muscle strips were frozen with a rapid-release

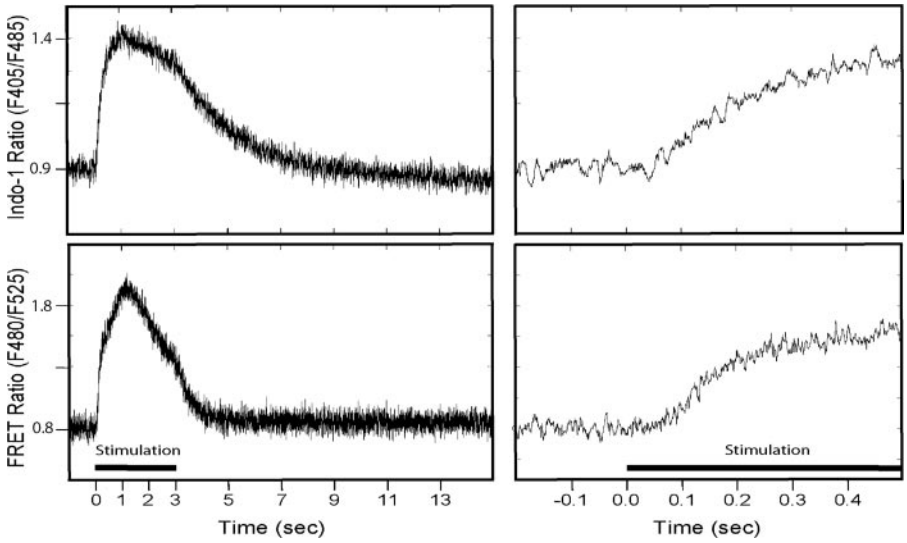

FIGURE 1. **Fluorescence ratio data for Indo-1 and MLCK CaM-sensor.** Traces are derived from the average values obtained from a single strip for repeated contractions to 50 Hz for 3 s, as indicated by the *stimulation bar*. *Right column* is the expanded time scale to illustrate latency.

electronic freezing device with hammer surfaces pre-chilled in liquid nitrogen (33). For the relaxation period, urinary bladder strips were frozen at 2, 5, 7, or 12 s after a 3-s electric field stimulation with the freezing device. Frozen samples were stored at −80 °C until they were added to a frozen slurry of acetone in 10% trichloroacetic acid, thawed, homogenized in 10% trichloroacetic acid and 10 mM dithiothreitol, and then centrifuged to process for protein phosphorylation measurements.

Measurement of RLC and CPI-17 Phosphorylation—Muscle proteins precipitated in 10% trichloroacetic acid and 10 mM dithiothreitol were solubilized in 8 M urea sample buffer and subjected to urea/glycerol-PAGE at 400 volts for 80 min (RLC) or 150 min (CPI-17) to separate non-phosphorylated and monophosphorylated protein forms (14, 34). Following electrophoresis, proteins were transferred to nitrocellulose membranes and probed with polyclonal antibodies against smooth muscle RLC or CPI-17. The ratio of monophosphorylated RLC or CPI-17 to total RLC or CPI-17 (nonphosphorylated plus monophosphorylated) was determined by quantitative densitometry and expressed as mole of phosphate/mol of protein.

Measurement of MYPT1, MLCK, and Paxillin Phosphorylation—Protein samples prepared in urea sample buffer were added to 0.2 volumes of SDS sample buffer containing 250 mM Tris, pH 6.8, 10% SDS, 50 mM dithiothreitol, 40% glycerol, and 0.01% bromphenol blue, boiled, and subjected to SDS-PAGE. Proteins were transferred to nitrocellulose membranes and visualized by immunoblot staining using antibodies to total MYPT1 and phospho-MYPT1 at Thr-696 or Thr-850 (Upstate, Waltham, MA); total MLCK (Sigma) and phospho-MLCK at Ser-1760 in the CaM-binding sequence (numbering for human MLCK sequence) (Invitrogen); and total paxillin (BD Biosciences) and phospho-paxillin at Tyr-118 (Cell Signaling Technology, Danvers, MA). The phosphorylation of MYPT1 and paxillin are expressed as a ratio relative to that obtained with tissues treated with 10 μM carbachol for 1 or 5 min, respectively, whereas MLCK phosphorylation is relative to results obtained with 65 mM KCl for 1 min.

Statistical Analyses—All data are presented as mean ± S.E. Statistical comparisons were performed by paired Student's t test for $[Ca^{2+}]_i$, MLCK activation, and force development, independent t test for phosphorylation of RLC, CPI-17, MYPT1, paxillin, and MLCK. Two-tailed values were used and p values <0.05 were considered significant.

RESULTS

Time Course for Increases in $[Ca^{2+}]_i$, MLCK Activation, RLC Phosphorylation, and Force with Neural Stimulation—Experiments were performed to optimize stimulus parameters such as strength, duration, or frequency for selective stimulation of intramural nerves in strips of mouse urinary bladder (26). Selected parameters were 20 V, 0.5 ms duration, 50 Hz direct current pulses to the muscle chamber to induce maximal contractile responses that were inhibited 57 ± 7% ($n = 5$) by the muscarinic antagonist 0.1 μM atropine. The neurally mediated contractile responses were inhibited 28 ± 5% ($n = 5$) with a combination of purinergic antagonists suramin and α,β-methylene ATP (10 μM each), whereas the addition of antagonists of both receptors inhibited contraction 93 ± 2% ($n = 10$). The contractile responses to neural stimulation were 1.45 ± 0.18 times the maximal response obtained with carbachol. These results are similar to previous reports on mouse bladder smooth muscle (29, 30) indicating the robust neural responses are mediated by both muscarinic and purinergic receptors.

For fluorescence studies and contractile measurements during neural stimulation, data were acquired continuously for 15 s. In Fig. 2*A*, the time for the onset of force development is illustrated in a typical tracing, whereas Fig. 2*B* shows contraction-relaxation responses over 15 s. Representative tracings of the Indo-1 ratio (F405/F485), FRET ratio (F480/F525), and force are shown in Fig. 2*C*. Measurements of neurally stimulated bladder smooth muscle strips demonstrated that $[Ca^{2+}]_i$ and MLCK activation increased rapidly upon electric field stimulation, whereas force development lagged, reaching its maximal response more gradually (Fig. 2*C*). During the relaxation phase following a 3-s stimulation, MLCK activation declined faster than $[Ca^{2+}]_i$ (Figs. 1 and 2*C*). Phosphorylation of RLC was measured in quick-frozen muscle samples at the indicated times by urea-glycerol PAGE (Fig. 2*D*). RLC phosphorylation was low in the nonstimulated bladder smooth muscle and increased rapidly with neural stimulation (0.11 ± 0.08 to 0.51 ± 0.06 mol of P/mol of RLC), consistent with the rapid MLCK activation.

There were significant changes in $[Ca^{2+}]_i$, MLCK activation, and force within the first 250 ms of neural stimulation (Fig. 3). Latencies for the onset of $[Ca^{2+}]_i$ and MLCK activation were

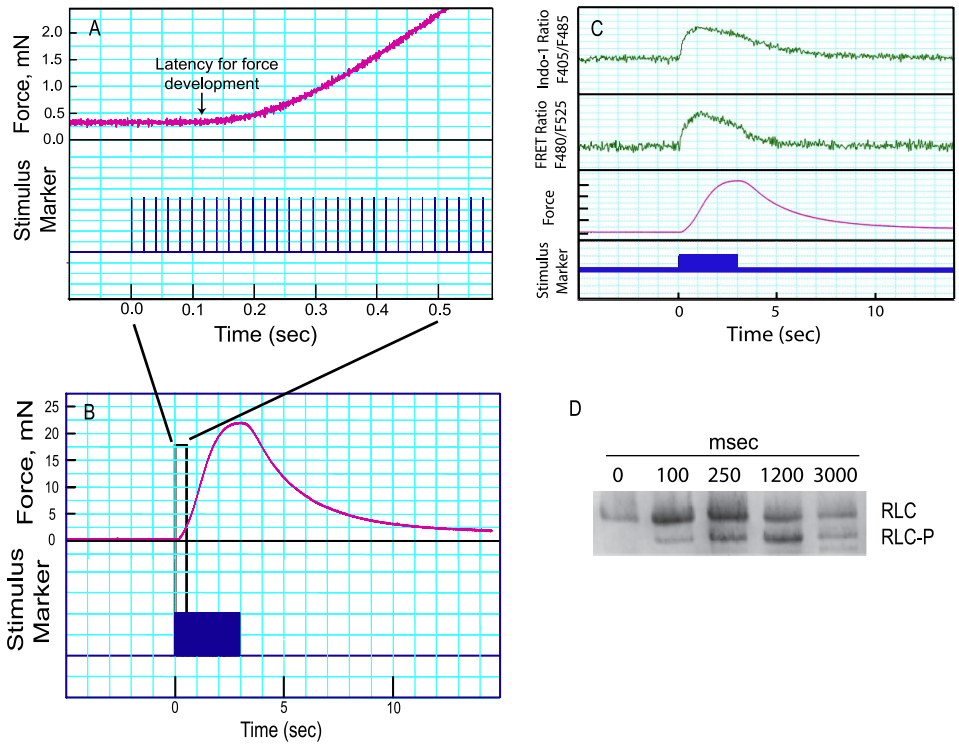

FIGURE 2. **Measurements of isometric force, Indo-1 ratio, FRET ratio, and RLC phosphorylation in electrically stimulated bladder smooth muscle strips.** *A*, representative force tracing (*upper channel*) upon electric field stimulation (*lower channel*) during the initial 0.5-s stimulation of a bladder strip from a CaM-sensor transgenic mouse. Stimulus pulses were delivered at 50 Hz. *Arrow* indicates the estimated time of latency for force development. Initiation of the stimulus train is designated time 0. *B*, representative force tracing for a 3-s electric field stimulation followed by 12 s relaxation. The response within the *black rectangle* was amplified to show the latency for force development in *A*. *C*, recordings of Indo-1 ratio, FRET ratio, and force responses in bladder strips stimulated for 3 s as indicated by the stimulus marker. Indo-1 ratio and FRET ratio are representative single traces from 2 strips filtered at 50 Hz. *D*, immunoblot following urea/glycerol-PAGE to separate phosphorylated RLC (*RLC-P*) from the nonphosphorylated RLC for strips frozen at the indicated times after the onset of stimulation.

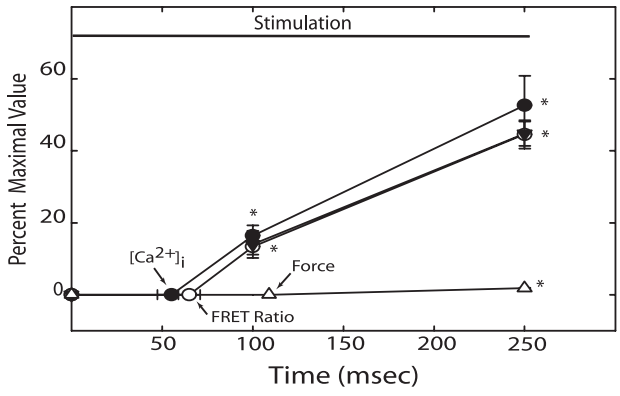

FIGURE 3. **Latencies and time course of $[Ca^{2+}]_i$, FRET ratio, RLC phosphorylation, and force during the initial 250 ms of electrical stimulation.** Values of $[Ca^{2+}]_i$ (●), FRET ratio (○), RLC phosphorylation (▼), and force (Δ) at the indicated times are expressed as a fraction of maximal values obtained with electric field stimulation. *Arrows* indicate average times for latency of the indicated parameter. Values are mean ± S.E. ($n = 4$ to 9). *, $p < 0.05$ *versus* resting value.

not significantly different ($p = 0.33$) at 55 ± 8 and 65 ± 6 ms, respectively (indicated by *arrows* in Fig. 3). Both $[Ca^{2+}]_i$ and MLCK activation increased rapidly following their respective latencies, and RLC phosphorylation was significantly elevated by 100 ms. Latency for the onset of force was significantly longer at 109 ± 3 ms. In addition, beyond the absolute latency, force increased considerably more slowly than RLC phosphorylation (Fig. 3). Delays due to coupling between $[Ca^{2+}]_i$ and MLCK activation appear insignificant.

$[Ca^{2+}]_i$, MLCK activation, and RLC phosphorylation responses continued to increase rapidly after 250 ms, reaching maximal values at 1.2 s (Fig. 4). $[Ca^{2+}]_i$ and RLC phosphorylation remained at maximal values up to 3 s, whereas MLCK activation partially decreased. Isometric force developed more slowly, reaching a maximal value after 3 s of stimulation. The times required for one-half maximal responses for $[Ca^{2+}]_i$, MLCK activation, and RLC phosphorylation were similar (250 ms), whereas force development was slower (1200 ms).

MYPT1, CPI-17, and Paxillin Phosphorylation—MYPT1 and CPI-17 phosphorylation play important roles in modulation of RLC phosphorylation and Ca^{2+} sensitization by inhibiting myosin light chain phosphatase activity (12, 14). Because MLCK activation decreased at 3 s without a significant decrease in RLC phosphorylation, we measured $MYPT1^{Thr\text{-}696}$, $MYPT1^{Thr\text{-}850}$, and CPI-17 phosphorylation (Fig. 5). We previously showed that treatment of mouse bladder tissues with 10 μM carbachol for 1 min significantly increased phosphorylation of $MYPT1^{Thr\text{-}696}$ and CPI-17 (14). In the present study, we used this treatment as a positive control for analysis. Compared with values obtained without neural stimulation, phosphorylation of $MYPT1^{Thr\text{-}850}$ and CPI-17 did not change up to 3 s (Fig. 5). $MYPT1^{Thr\text{-}696}$ did not change significantly until 3 s. However, in smooth muscle tissues that were stimulated an additional 2 s (5 s total) there were significant increases in $MYPT1^{Thr\text{-}696}$ and $MYPT1^{Thr\text{-}850}$ phosphorylation that were similar to values obtained with carbachol stimulation for 1 min (108 ± 15 and 79 ± 5%, respectively). There was no increase in CPI-17 phosphorylation at 5 s of neural stimulation (22 ± 2%). These data indicate that phosphorylations of MYPT1 and CPI-17 do not play a significant role in the initial contractile response of bladder smooth muscle to neural stimulation.

Paxillin at membrane adhesions undergoes tyrosine phosphorylation concurrently with force development with agonist. This response is thought to play a role in the polymerization of submembranous cytoskeletal actin filaments that increases the rigidity of the membrane during tension development and allows force transmission of phosphorylated, cycling myosin cross-bridges (20). Therefore, we also measured paxillin phosphorylation in response to neural stimulation (Fig. 5). Relative

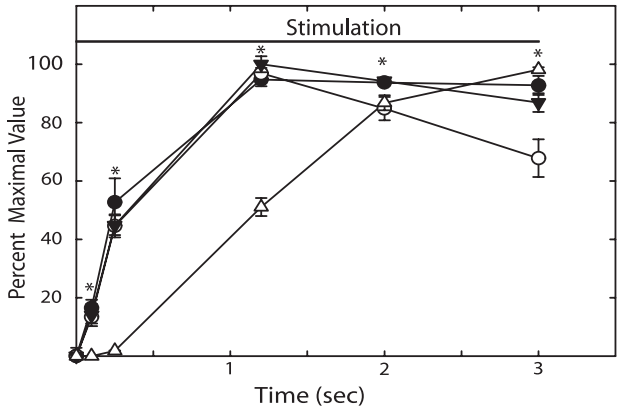

FIGURE 4. **Time course of $[Ca^{2+}]_i$, FRET ratio, RLC phosphorylation, and force during 3 s of electrical stimulation.** Values of $[Ca^{2+}]_i$ (●), FRET ratio (○), RLC phosphorylation (▼), and force (Δ) at the indicated times are expressed as a fraction of maximal obtained with electric field stimulation. Values are mean ± S.E. ($n = 5$ to 12). *, $p < 0.05$ *versus* resting values (all values significantly changed at each time after 0 s as shown by *one asterisk* for each time).

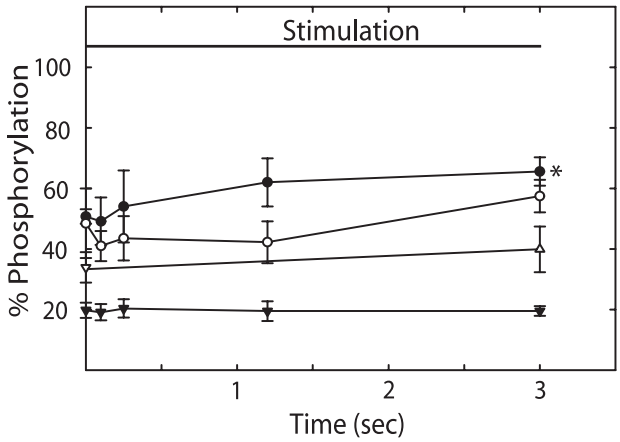

FIGURE 5. **MYPT1$^{Thr\text{-}696}$, MYPT1$^{Thr\text{-}850}$, CPI-17, and paxillin phosphorylation during 3 s of electrical stimulation.** MYPT1$^{Thr\text{-}696}$ (●), MYPT1$^{Thr\text{-}850}$ (○), CPI-17 (▼), and paxillin (Δ) phosphorylation at the indicated times during a 3-s field stimulation. For MYPT1$^{Thr\text{-}696}$, MYPT1$^{Thr\text{-}850}$, and paxillin phosphorylation, results are expressed relative to values obtained with 10 μM carbachol at 1 (MYPT1) and 5 (paxillin) min. For CPI-17 phosphorylation, results are expressed as percent of total CPI phosphorylated (14). Values are mean ± S.E. ($n = 4$ to 6). *, $p < 0.05$ *versus* resting values.

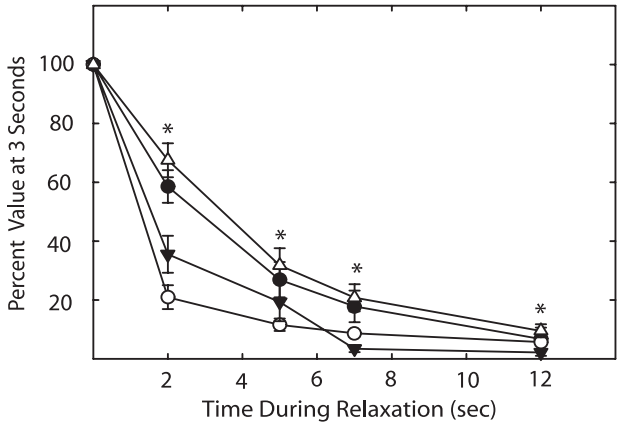

FIGURE 6. **$[Ca^{2+}]_i$, FRET ratio, RLC phosphorylation, and force during relaxation after 3 s of electrical stimulation.** Strips were frozen at the indicated times during relaxation. Values of $[Ca^{2+}]_i$ (●), FRET ratio (○), RLC phosphorylation (▼), and force (Δ) are expressed as percent of values at 3 s. Values are mean ± S.E. ($n = 4$ to 9). *, $p < 0.05$ *versus* resting values (all values significantly changed after 0 s as shown by *one asterisk* for each time).

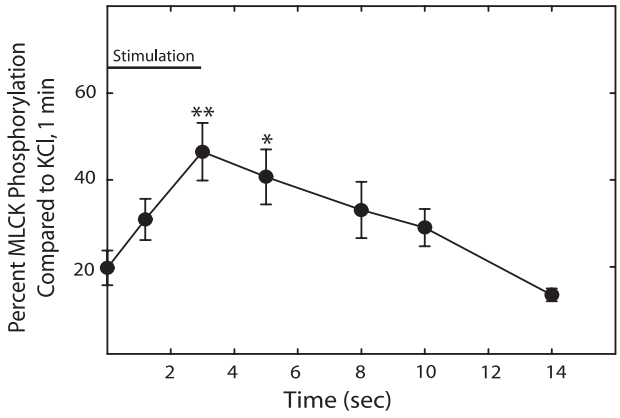

FIGURE 7. **MLCK phosphorylation during contraction and relaxation with electrical stimulation.** Results are expressed relative to values obtained at 1 min with 65 mM KCl. Values are mean ± S.E. ($n = 4$ to 8). *, $p < 0.05$ *versus* resting value. **, $p < 0.01$ *versus* resting values.

to the phosphorylation response with carbachol, there was no significant increase in paxillin phosphorylation by 3 s of neural stimulation.

$[Ca^{2+}]_i$, MLCK Activation, RLC Phosphorylation, and Force during Relaxation—After stimulating smooth muscle tissues for 3 s, responses were measured during the subsequent relaxation period; values were normalized to the values obtained at 3 s of stimulation (Fig. 6). The extent of MLCK activation declined rapidly, whereas $[Ca^{2+}]_i$ declined more slowly. Force declined more slowly than RLC phosphorylation. Estimated half-times for decreases in $[Ca^{2+}]_i$, MLCK activation, and force during the relaxation phase from the continuous measurements were 2.6 ± 0.4, 0.7 ± 0.9, and 3.2 ± 0.6 s, respectively. The estimated half-time for RLC dephosphorylation is at least 1.2 s.

MLCK Phosphorylation—Ca^{2+}-dependent phosphorylation of MLCK has been implicated in a Ca^{2+} desensitization mechanism by inhibiting Ca^{2+}/CaM binding to the kinase (35, 36). Because there was a decline in MLCK activation before an apparent decline in $[Ca^{2+}]_i$ during the contraction and relaxation periods, MLCK phosphorylation was measured by Western blotting with an antibody that binds to the phosphorylated serine in the C terminus of the Ca^{2+}/CaM binding sequence in MLCK that affects Ca^{2+}/CaM binding. Depolarization of smooth muscle tissues with high concentrations of K^+ leads to increased MLCK phosphorylation (17, 35). Therefore, we treated smooth muscle tissues with 65 mM KCl for 1 min as a positive control. In the neurally stimulated tissues, MLCK phosphorylation reached a maximal response by 3 s and then gradually declined to resting values during the relaxation period (Fig. 7). The decrease in MLCK activation while $[Ca^{2+}]_i$ remained elevated during neural stimulation and in the early phase of relaxation correlates to MLCK phosphorylation.

DISCUSSION

The principal finding of the present study is that physiological stimulation of bladder smooth muscle by neurotransmitter

release results in rapid increases in $[Ca^{2+}]_i$, MLCK activation, and RLC phosphorylation revealing the activity of a tightly coupled signaling complex that precedes isometric force development. The electrical stimulation paradigm used in this study was selected to approximate the time course of mouse bladder contractions measured by filling cystometry *in vivo* (37, 38). Similar to the response pattern in isolated muscle, pressure traces from intact bladder during voiding show a rapid contraction lasting just a few seconds, followed by a slower relaxation taking 10 or more seconds. Our results are similar to those of others where electric field stimulation of mouse bladder smooth muscle strips elicits rapid, frequency-dependent contractions that are maximal at 50 Hz and that are inhibited ~60% by muscarinic and ~30% by purinergic antagonists (30, 39). These maximal stimulus conditions resulted in increases in intracellular Ca^{2+} at rates similar to those measured in postsynaptic responses of detrusor muscle from Ca^{2+}-sensing mice (40). We have not identified the sources of calcium in response to maximal neural stimulation, however, the importance of Ca^{2+} entry through voltage-dependent calcium channels for normal bladder function was clearly demonstrated with the smooth muscle-specific knock-out of the $Ca_v1.2$ L-type calcium channel (41). Both muscarinic and purinergic agonists have been shown to elicit depolarization of mouse bladder smooth muscle (42). Thus, the minimal signaling through RhoA or PKC pathways, evidenced by slight or no changes in MYPT1 and CPI-17 phosphorylation during short cycles of contraction, may reflect the predominance of calcium signaling in regulating normal bladder function.

MLCK has a high affinity for Ca^{2+}/CaM with an apparent K_D value of 1 nM (43). Ca^{2+} binds to CaM quite rapidly (1×10^8 M^{-1} s^{-1}) to induce conformational changes necessary for its binding to MLCK, which occurs as a rapid, bimolecular association (5×10^7 M^{-1} s^{-1}) (44–46). This binding is associated with a slower conformational isomerization (~2 s^{-1}) of skeletal as well as smooth muscle MLCK in the binary complex. Although skeletal muscle myosin light chain kinase activation occurs more rapidly than the slower structural isomerization (45), similar evidence is lacking for smooth muscle MLCK leading others to propose that the isomerization process could account in part for the latency of contraction in stimulated smooth muscles (46). However, the activation of smooth muscle MLCK in the neurally stimulated tissues was tightly coupled with the increase in $[Ca^{2+}]_i$. The latencies for $[Ca^{2+}]_i$ and MLCK activation were not different at 55 and 65 ms, respectively. To estimate the rates of rise for $[Ca^{2+}]_i$ and MLCK activation, the rising segment, between 0.1 and 1.2 s, was fit by a one-phase exponential ($r^2 > 0.99$). The pseudo-first order rates were similar at 2.4 and 3.0 s^{-1}, respectively. Therefore, we conclude that there is no significant delay in Ca^{2+}/CaM binding and activation of smooth muscle MLCK, *in vivo*. This conclusion is similar to results obtained biochemically (45) and physiologically (47) with skeletal muscle MLCK.

Changes in $[Ca^{2+}]_i$ do not always lead to proportional increases in MLCK activation. At longer times after initiation of neural stimulation, there was an apparent desensitization of the kinase to Ca^{2+}. This desensitization occurs when MLCK is phosphorylated in the C terminus of its CaM binding sequence that would decrease the affinity of the kinase for Ca^{2+}/CaM (17, 35). The phosphorylation was shown previously to be Ca^{2+}-dependent (17, 18) and recent evidence indicates it may be mediated by Ca^{2+}-dependent activation of CaM-dependent protein kinase kinase-β that phosphorylates and activates AMP-activated protein kinase, which then phosphorylates MLCK (19). If the concentration of AMP increases sufficiently in contracting muscle, it may also directly activate AMP-activated protein kinase. The Ca^{2+}-dependent or AMP-stimulated feedback mechanisms would thus diminish MLCK activity.

The activation of MLCK is tightly coupled to RLC phosphorylation. With the initiation of contraction, there were proportional increases in the extent of MLCK activation and RLC phosphorylation up to 3 s. The initial characterization of the CaM-sensor MLCK showed a proportional change in FRET ratio with kinase activity when equilibrated at different calcium concentrations (31). The physiological data herein show that the rates of change in FRET ratio and RLC phosphorylation are similar. After cessation of neural stimulation, there were decreases in $[Ca^{2+}]_i$, MLCK activation, and RLC phosphorylation within a few seconds resulting in relaxation. The decreases in MLCK activation and RLC phosphorylation appeared to precede decreases in $[Ca^{2+}]_i$ probably because of the Ca^{2+} desensitization of MLCK by the phosphorylation of its CaM binding sequence.

Neural stimulation did not result in activation of Ca^{2+}-sensitization pathways involving G protein receptor coupling signaling through RhoA or PKC to phosphorylation of MYPT1 or CPI-17 within the time required for maximal force development. Ca^{2+}-sensitization has been noted in a variety of smooth muscle tissues where it is thought to play physiological as well as pathophysiological roles (12, 13, 15). We did not observe phosphorylation of MYPT1 or CPI-17 during neural stimulation up to 3 s, consistent with the view that Ca^{2+}-dependent RLC phosphorylation initiates smooth muscle contraction with Ca^{2+}-sensitization mechanisms recruited later as important but secondary modulatory events. Carbachol stimulation with its associated slower contractile response does lead to MYPT1 and CPI-17 phosphorylation in bladder smooth muscle (14, 48) as it does for other kinds of smooth muscles (12, 13, 15). However, the primary importance of MLCK for phasic smooth muscle contraction even with agonist stimulation is emphasized by the loss of contractile responses with MLCK gene ablation (3). Because of the tight temporal link between MLCK activation and RLC phosphorylation, it also appears that Ca^{2+}-independent kinases are not involved in RLC phosphorylation with neural stimulation. Similarly, ablation of the MLCK gene did not uncover Ca^{2+}-independent RLC phosphorylation in bladder smooth muscle (3).

Evidence has also been presented that smooth muscle contraction requires the polymerization of submembranous cytoskeletal actin filaments that increases the rigidity of the membrane during tension development (20–23). These changes may strengthen membrane adhesion complexes and allow transmission of forces from cycling cross-bridges of myosin on actin through the adhesion complexes to the external force transmitting structures. Thus, signals activated by integrin receptors and G protein-coupled receptors collaborate to

regulate actin cytoskeletal remodeling as well as activation of actomyosin. These two processes can be activated independently of one another, but it is proposed that the development of contractile force requires the activation of both the actomyosin system and actin polymerization (20). One of the first steps in initiating cytoskeletal remodeling in response to agonist stimulation is the tyrosine phosphorylation of paxillin that recruits it to membrane adhesion sites to facilitate the adaptation of smooth muscle cell shape and stiffness. We did not observe a change in paxillin phosphorylation during neural stimulation, similar to our observations on MYPT1 and CPI-17 phosphorylation. Recent observations on vascular smooth muscle show that paxillin phosphorylation follows, rather than precedes force development (49). Thus, paxillin phosphorylation and cytoskeletal remodeling may be recruited after the primary RLC phosphorylation and force development responses for increasing cell force. Alternatively, the neural stimulus may activate a different pathway for actin polymerization or cytoskeletal remodeling may play a more important role in other kinds of smooth muscles such as tonic airway smooth muscle compared with phasic bladder smooth muscle.

The relationship between RLC phosphorylation and force with neural stimulation is complex and shows considerable hysteresis in the contraction and relaxation phases. In skinned fibers and in intact tissue strips at peak force, there is a relatively simple relationship where force is proportional to RLC phosphorylation (14, 50). However, rapid cell activation by neurotransmitter released during electric field stimulation of nerves shows a significant lag between RLC phosphorylation and force during force development and a greater rate of RLC dephosphorylation relative to force during relaxation (26). Force developed by the cyclic interactions between myosin and actin is transmitted through elastic elements located in the tissue, cells, and contractile apparatus. Thus, the delay in force during contraction relative to rapid RLC phosphorylation is most likely attributable to the effects of internal compliance on the manifestation of force in the tissue (51).

In summary, neural stimulation of a phasic smooth muscle tissue leads to rapid increases in $[Ca^{2+}]_i$, MLCK activation, and RLC phosphorylation, showing a tightly coupled Ca^{2+} signaling complex as an elementary cellular response sufficient to initiate contraction. Modulatory signaling pathways involving Ca^{2+}-sensitization via inhibition of myosin phosphatase activity (MYPT1 and CPI-17 phosphorylation) or Ca^{2+}-independent kinases were not evident.

REFERENCES

1. Kamm, K. E., and Stull, J. T. (1985) *Annu. Rev. Pharmacol. Toxicol.* **25,** 593–620
2. Somlyo, A. P., and Somlyo, A. V. (2000) *J. Physiol.* **522,** 177–185
3. He, W. Q., Peng, Y. J., Zhang, W. C., Lv, N., Tang, J., Chen, C., Zhang, C. H., Gao, S., Chen, H. Q., Zhi, G., Feil, R., Kamm, K. E., Stull, J. T., Gao, X., and Zhu, M. S. (2008) *Gastroenterology* **135,** 610–620
4. Tansey, M. G., Luby-Phelps, K., Kamm, K. E., and Stull, J. T. (1994) *J. Biol. Chem.* **269,** 9912–9920
5. Zimmermann, B., Somlyo, A. V., Ellis-Davies, G. C., Kaplan, J. H., and Somlyo, A. P. (1995) *J. Biol. Chem.* **270,** 23966–23974
6. Isotani, E., Zhi, G., Lau, K. S., Huang, J., Mizuno, Y., Persechini, A., Geguchadze, R., Kamm, K. E., and Stull, J. T. (2004) *Proc. Natl. Acad. Sci. U. S. A.* **101,** 6279–6284
7. Ito, M., Nakano, T., Erdodi, F., and Hartshorne, D. J. (2004) *Mol. Cell. Biochem.* **259,** 197–209
8. Hirano, K., Derkach, D. N., Hirano, M., Nishimura, J., and Kanaide, H. (2003) *Mol. Cell. Biochem.* **248,** 105–114
9. Ihara, E., Moffat, L., Ostrander, J., Walsh, M. P., and MacDonald, J. A. (2007) *Am. J. Physiol. Gastrointest. Liver Physiol.* **293,** G699–710
10. Deng, J. T., Van Lierop, J. E., Sutherland, C., and Walsh, M. P. (2001) *J. Biol. Chem.* **276,** 16365–16373
11. Wibberley, A., Chen, Z., Hu, E., Hieble, J. P., and Westfall, T. D. (2003) *Br. J. Pharmacol.* **138,** 757–766
12. Somlyo, A. P., and Somlyo, A. V. (2003) *Physiol. Rev.* **83,** 1325–1358
13. Ihara, E., and MacDonald, J. A. (2007) *Can. J. Physiol. Pharmacol.* **85,** 79–87
14. Mizuno, Y., Isotani, E., Huang, J., Ding, H., Stull, J. T., and Kamm, K. E. (2008) *Am. J. Physiol. Cell Physiol.* **295,** C358–364
15. Murthy, K. S. (2006) *Annu. Rev. Physiol.* **68,** 345–374
16. Kitazawa, T., Eto, M., Woodsome, T. P., and Brautigan, D. L. (2000) *J. Biol. Chem.* **275,** 9897–9900
17. Stull, J. T., Hsu, L. C., Tansey, M. G., and Kamm, K. E. (1990) *J. Biol. Chem.* **265,** 16683–16690
18. Tansey, M. G., Word, R. A., Hidaka, H., Singer, H. A., Schworer, C. M., Kamm, K. E., and Stull, J. T. (1992) *J. Biol. Chem.* **267,** 12511–12516
19. Horman, S., Morel, N., Vertommen, D., Hussain, N., Neumann, D., Beauloye, C., El Najjar, N., Forcet, C., Viollet, B., Walsh, M. P., Hue, L., and Rider, M. H. (2008) *J. Biol. Chem.* **283,** 18505–18512
20. Gunst, S. J., and Zhang, W. (2008) *Am. J. Physiol. Cell Physiol.* **295,** C576–587
21. Turner, C. E. (2000) *Nat. Cell Biol.* **2,** E231–236
22. Wang, Z., Pavalko, F. M., and Gunst, S. J. (1996) *Am. J. Physiol. Cell Physiol.* **271,** C1594–1602
23. Mehta, D., Wang, Z., Wu, M. F., and Gunst, S. J. (1998) *Am. J. Physiol. Cell Physiol.* **274,** C741–747
24. Gunst, S. J., Tang, D. D., and Opazo Saez, A. (2003) *Respir. Physiol. Neurobiol.* **137,** 151–168
25. Opazo Saez, A., Zhang, W., Wu, Y., Turner, C. E., Tang, D. D., and Gunst, S. J. (2004) *Am. J. Physiol. Cell Physiol.* **286,** C433–447
26. Kamm, K. E., and Stull, J. T. (1985) *Am. J. Physiol. Cell Physiol.* **249,** C238–247
27. Persechini, A., Kamm, K. E., and Stull, J. T. (1986) *J. Biol. Chem.* **261,** 6293–6299
28. Silinsky, E. M., and Redman, R. S. (1996) *J. Physiol.* **492,** 815–822
29. Heppner, T. J., Bonev, A. D., and Nelson, M. T. (2005) *J. Physiol.* **564,** 201–212
30. Werner, M. E., Knorn, A. M., Meredith, A. L., Aldrich, R. W., and Nelson, M. T. (2007) *Am. J. Physiol. Regul. Integr. Comp. Physiol.* **292,** R616–624
31. Geguchadze, R., Zhi, G., Lau, K. S., Isotani, E., Persechini, A., Kamm, K. E., and Stull, J. T. (2004) *FEBS Lett.* **557,** 121–124
32. Agbulut, O., Huet, A., Niederländer, N., Puceat, M., Menasché, P., and Coirault, C. (2007) *J. Biol. Chem.* **282,** 10465–10471
33. Thompson, C. I., Rubio, R., and Berne, R. M. (1980) *Am. J. Physiol. Heart Circ. Physiol.* **238,** H389–398
34. Kamm, K. E., Hsu, L. C., Kubota, Y., and Stull, J. T. (1989) *J. Biol. Chem.* **264,** 21223–21229
35. Stull, J. T., Tansey, M. G., Tang, D. C., Word, R. A., and Kamm, K. E. (1993) *Mol. Cell. Biochem.* **127–128,** 229–237
36. Kamm, K. E., and Stull, J. T. (2001) *J. Biol. Chem.* **276,** 4527–4530
37. Pandita, R. K., Fujiwara, M., Alm, P., and Andersson, K. E. (2000) *J. Urol.* **164,** 1385–1389
38. Chen, Q., Takahashi, S., Zhong, S., Hosoda, C., Zheng, H. Y., Ogushi, T., Fujimura, T., Ohta, N., Tanoue, A., Tsujimoto, G., and Kitamura, T. (2005) *J. Urol.* **174,** 370–374
39. Ekman, M., Andersson, K. E., and Arner, A. (2006) *Eur. J. Pharmacol.* **532,** 99–106
40. Ji, G., Feldman, M. E., Deng, K. Y., Greene, K. S., Wilson, J., Lee, J. C., Johnston, R. C., Rishniw, M., Tallini, Y., Zhang, J., Wier, W. G., Blaustein, M. P., Xin, H. B., Nakai, J., and Kotlikoff, M. I. (2004) *J. Biol. Chem.* **279,** 21461–21468
41. Wegener, J. W., Schulla, V., Lee, T. S., Koller, A., Feil, S., Feil, R., Kleppisch,

T., Klugbauer, N., Moosmang, S., Welling, A., and Hofmann, F. (2004) *FASEB J.* **18,** 1159–1161
42. Meng, E., Young, J. S., and Brading, A. F. (2008) *Neurourol. Urodynamics* **27,** 79–87
43. Stull, J. T., Nunnally, M. H., and Michnoff, C. H. (1986) in *The Enzymes* (Krebs, E. G., and Boyer, P. D., eds) pp. 113–166, Academic Press, Orlando, FL
44. Johnson, J. D., Holroyde, M. J., Crouch, T. H., Solaro, R. J., and Potter, J. D. (1981) *J. Biol. Chem.* **256,** 12194–12198
45. Bowman, B. F., Peterson, J. A., and Stull, J. T. (1992) *J. Biol. Chem.* **267,** 5346–5354
46. Török, K., and Trentham, D. R. (1994) *Biochemistry* **33,** 12807–12820
47. Ryder, J. W., Lau, K. S., Kamm, K. E., and Stull, J. T. (2007) *J. Biol. Chem.* **282,** 20447–20454
48. Gomez-Pinilla, P. J., Gomez, M. F., Swärd, K., Hedlund, P., Hellstrand, P., Camello, P. J., Andersson, K. E., and Pozo, M. J. (2008) *J. Pineal Res.* **44,** 416–425
49. Rembold, C. M., Tejani, A. D., Ripley, M. L., and Han, S. (2007) *Am. J. Physiol. Cell Physiol.* **293,** C993–1002
50. Kenney, R. E., Hoar, P. E., and Kerrick, W. G. (1990) *J. Biol. Chem.* **265,** 8642–8649
51. Aksoy, M. O., Mras, S., Kamm, K. E., and Murphy, R. A. (1983) *Am. J. Physiol. Cell Physiol.* **245,** C255–270